Assessment of a Combined QM/MM Approach for the Study of Large Nitroxide Systems in Vacuo and in Condensed Phases

Vincenzo Barone,*,† Alessandro Bencini,‡ Maurizio Cossi,† Andrea Di Matteo,† Maurizio Mattesini,‡ and Federico Totti‡

Contribution from the Dipartimento di Chimica, Universita' Federico II, via Mezzocannone 4, I-80134 Napoli, Italy, and the Dipartimento di Chimica, Universita' di Firenze, via Maragliano 75, I-50144 Firenze, Italy

Received March 31, 1998

Abstract: The structures and spectromagnetic properties of some model nitroxides were studied by a self-consistent hybrid of Hartree−Fock and density functional methods (B3LYP) obtaining results close to experimental data. From the computed structures, together with the available experimental data, new parameters for the NO moiety have been derived for two of the most commonly used force fields, namely, the MM+ and the universal force field. This provides the background for computations of reliable structures and spectromagnetic observables of large nitroxide systems. As examples of applications we report the following: (a) the structure of 2,2,5,5-tetramethyl-3-hydroxypyrrolidine-1-oxyl radical (PROXYL) optimized in the gas phase and in the crystalline solid; (b) the calculation of the magnetic exchange coupling constant of the large organic biradical 1,4-bis(4′,4′-dimethyloxazolidine-*N*-oxyl)cyclohexane (OXYL) using geometries optimized by the new force field; (c) solvent effects on the hyperfine properties of representative nitroxides computed by a discrete-continuum model using structural parameters optimized by the new force field for the solute and for its first solvation shell. Geometry optimizations with the new force fields always give structures in good agreement with the experiment both in vacuo and in condensed phases (solution and crystalline solid). Using these structures, remarkably accurate spectromagnetic observables are obtained by the combined use of the B3LYP method and of the polarizable continuum model for the description of bulk solvent effects.

Introduction

Nitroxides are one of the few classes of organic free radicals that are stable under ordinary conditions.[1] This has allowed the determination of a number of molecular structures by using X-ray crystallographic methods and the consequent unequivocal correlation between structural and spectroscopic parameters.[2] This characteristic, coupled to the strong localization of the unpaired spin in the NO moiety,[3] makes nitroxides ideal "Spin Labels" to explore the structure of short-lived free radicals[4−6] by electron spin resonance (ESR) spectroscopy.[7] From another point of view, several nitroxides and, especially, nitronyl nitroxides have been used in past few years as possible precursors for ferromagnetic materials, thus adding magnetic properties to the growing abundance of electrical and optical phenomena exhibited by organic molecular solids.[8] Only by obtaining total control of the relative orientations and of the intermolecular contacts of nitroxides in the crystal lattices will it be possible to govern the nature and dimensionality of the magnetic interactions and, therefore, to design new organic bulk ferromagnets with high and usable critical temperatures.[9] An efficient and reliable way of handling the structure of the radicals in the solid state appears therefore particularly appealing.

While detailed experimental information is available for the above systems, a number of aspects remain for which quantum mechanical studies can provide useful information. These involve, for instance, a clear-cut separation between the different effects (e.g., intrinsic and environmental) that contribute to the overall observables, or the relationship between molecular structure and spectromagnetic properties. Several studies have shown that refined post-Hartree−Fock (post-HF) and, more recently, density functional (DF) methods can provide remarkably accurate results.[10−20] Unfortunately, with highly reactive

* To whom correspondence should be addressed: (phone) +3981-5476503; (fax) +39818-5527771; (e-mail) enzo@chemna.dichi.unina.it.

† Università Federico II.

‡ Università di Firenze.

(1) Rassat, A. *Pure Appl. Chem.* **1990**, *62*, 223.

(2) (a) Capiomont, A.; Lajzerowicz-Bonneteau, J. *Acta Crystallogr.* **1971**, *B27*, 322. (b) Turley, J. W.; Boer, F. P. *Acta Crystallogr.* **1972**, *B28*, 618. (c) Lajzerowicz-Bonneteau, J. In *Spin Labeling, Theory and Applications*; Berliner, D., Ed.; Academic Press: New York, 1970; p 239.

(3) (a) Ricca, A.; Tronchet, J. M.; Weber, J.; Ellinger, Y. *J. Phys. Chem.* **1992**, *96*, 10779. (b) Bordeaux, D.; Boucherle, J. X.; Delley, B.; Gillon, B.; Ressouche, E.; Schweizer, J. In *Magnetic Molecular Materials*; Gatteschi, D., Kahn, O., Miller, J. S., Palacio, F., Eds.; NATO ASI Series; Kluwer: Dordrecht, 1991; p 371.

(4) (a) Hanson, P.; Lilhauser, G.; Formaggio, F.; Crisma, M.; Toniolo, C. *J. Am. Chem. Soc.* **1996**, *118*, 7618. (b) Keana, J. F. W. *Chem. Rev.* **1978**, *78*, 37.

(5) Janzen, E. G. *Acc. Chem. Res.* **1971**, *4*, 31.

(6) (a) Yamada, B.; Fujita, M.; Otsu, T. *Makromol. Chem.* **1991**, *192*, 1829. (b) Abe, K.; Suezawa, H.; Hirota, M.; Ishii, T. *J. Chem. Soc., Perkin Trans. 2* **1984**, 29.

(7) Tronchet, J. M. In *Bioactive Spin Labels*; Zhdanov, R. I., Ed.; Springer-Verlag: Berlin, 1992; p 355.

(8) (a) Chiarelli, R.; Novak, M. A.; Rassat, A.; Tholince, J. L. *Nature (London)* **1993**, *363*, 147. (b) Ciujeda, J.; Mas, M.; Molins, E.; Laufranc de Pauthou, F.; Laugier, J.; Park, J. G.; Paulsen, C.; Rey, P.; Rovira, C.; Veciana, J. *J. Chem. Soc., Chem. Commun.* **1995**, 709. (c) Caneschi, A.; Gatteschi, D.; Rey, P. *Prog. Inorg. Chem.* **1991**, *39*, 331.

(9) *Magnetic Molecular Materials*; Gatteschi, D., Kahn, O., Miller, J. S., Palacio, F., Eds.; NATO ASI Series E, 198; Kluwer: Dordrecht, 1991.

(10) Barone, V.; Lelj, F.; Russo, N.; Ellinger, Y.; Subra, R. *Chem. Phys.* **1983**, *76*, 385.

(11) Pauzat, F.; Gritli, H.; Ellinger, Y.; Subra, R. *J. Phys. Chem.* **1984**, *88*, 4581.

(12) Ellinger, Y.; Subra, R.; Rassat, A.; Douady, J.; Berthier, G. *J. Am. Chem. Soc.* **1975**, *97*, 476.

S0002-7863(98)01079-8 CCC: $15.00
Published on Web 07/07/1998

species, and particularly free radicals, it often occurs that the simplest representatives amenable to high-level quantum mechanical studies are too unstable to allow reliable experimental measurements, whereas the stable members of the series have gained their stability at the price of profound structural modifications which deeply affect the geometry of their nitroxide moiety.

An effective way out from this dilemma is provided by combined models in which reliable physicochemical properties are obtained through single-point computations by sophisticated quantum mechanical methods employing geometrical structures optimized by the much less expensive molecular mechanics (MM) techniques. However, the MM approach rests on the availability of simple and accurate force fields for the description of potential energy surfaces governing conformational transitions.[21] The combined use of experimental and quantum-mechanical reference data is particularly useful in the fitting of parameters,[22] especially for unstable species. We have recently followed this approach in the extension of current force fields to radical amino acid residues.[23] Here we try to further extend the range of applicability of molecular mechanics to systems containing nitroxide moieties paying particular attention to the role of environmental effects (i.e., solvent and crystal forces) in modifying structural features and spectromagnetic properties. To this end, we have used two of the most popular force fields, namely, MM+ and the universal force field (UFF), as implemented in the HyperChem and Cerius^2 program packages,[24,25] respectively. Our choice takes into account that the MM+ parametrization is derived and includes the Allinger MM2 force field, which is the most widely used in organic chemistry[26] whereas UFF represents one of the last generation force fields and can be applied to all the elements of the periodic table.[27]

The parametrization is based on a training set of four medium-size nitroxide radicals, which are representative of the different ranges of pyramidalization for the NO group. The structures of the radicals are sketched in Figure 1. In particular the bis-(*tert*-butyl) nitroxide (TBNO) and the 2,2,5,5-tetramethyl-3-hydroxypyrrolidine-1-oxyl (PROXYL) radicals are planar, whereas the 2,2,6,6-tetramethyl-4-piperidinol-1-oxyl) (TANOL) and the dimethyl nitroxide (MNO) radicals are significantly pyramidal.

As we shall see, reliable results in the gas phase or in inert matrixes are obtained by adding to standard force fields just two new atom types (referred to as NR and OR, respectively)

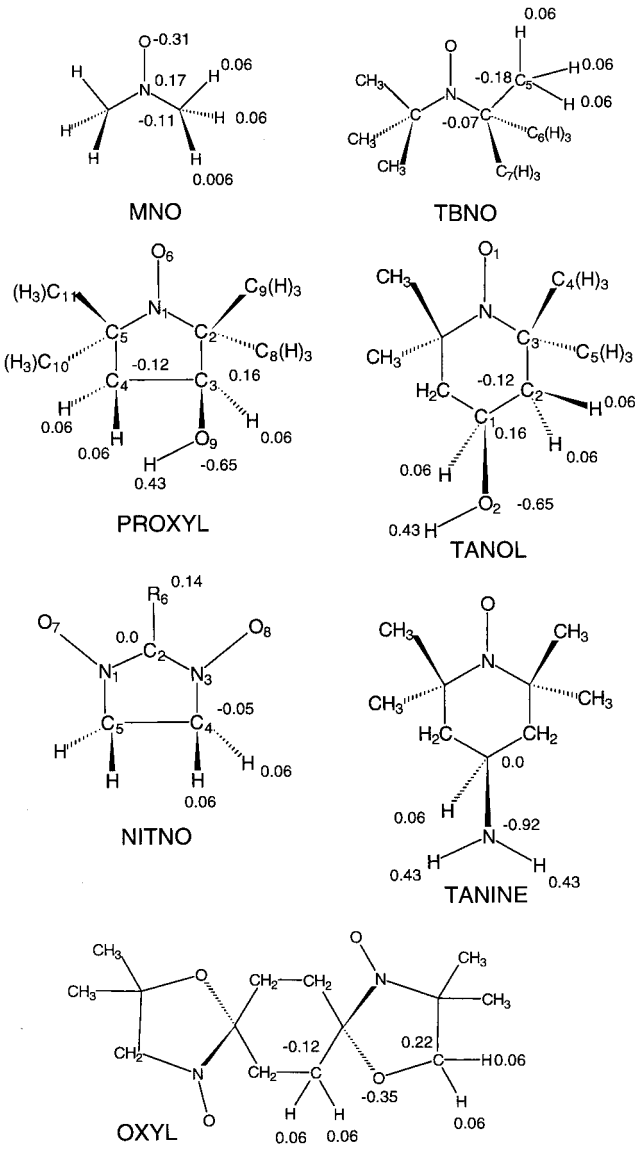

Figure 1. Structures, atom numbering, and net atomic charges of the nitroxides considered in the present work.

corresponding to the nitrogen and oxygen atoms of the nitroxide group. However, the simulation of nitroxide radicals in condensed phases requires a detailed description of interactions governing middle- and long-range intermolecular interactions such as van der Waals (VdW) forces and hydrogen bond interactions. The relevant parameters for these interactions were optimized by fitting the cell constants of representative nitroxides in the solid state.[28] Concerning solutions, we have recently shown that accurate properties can be computed using a combined discrete-continuum model, in which strongly bound solvent molecules are explicitly included, whereas bulk solvent effects are described by last-generation continuum models.[29] In the case of nitroxide radicals in aqueous solution, the NO moiety is strongly hydrated by two water molecules,[30] so that we have

(13) Barone, V. *J. Chem. Phys.* **1994**, *101*, 10666.
(14) (a) Barone, V.; Adamo, C.; Grand, A.; Brunel, Y.; Fontecave, M.; Subra, R. *J. Am. Chem. Soc.* **1995**, *117*, 1083. (b) Barone, V.; Adamo, C.; Grand, A.; Brunel, Y.; Jolibois, F.; Subra, R. *J. Am. Chem. Soc.* **1995**, *117*, 12618.
(15) Carmichael, I. *J. Phys. Chem.* **1991**, *95*, 108.
(16) Barone, V. In *Recent Advances in Density Functional Methods*; Chong, D. P., Ed.; World Scientific: Singapore, 1995; p 287.
(17) Adamo, C.; Barone, V.; Fortunelli, A. *J. Chem. Phys.* **1995**, *102*, 384.
(18) Barone, V. *Theor. Chim. Acta* **1995**, *91*, 113.
(19) Barone, V. *J. Phys. Chem.* **1995**, *99*, 11659.
(20) Barone, V.; Adamo, C. *Chem. Phys. Lett.* **1994**, *224*, 432.
(21) Burkert, U.; Allinger, N. L. *Molecular Mechanics*; ACS Monograph Series 177; American Chemical Society: Washington, DC, 1982.
(22) Cornell, W. D.; Cieplak, P.; Bayly, C. I.; Gould, I. R.; Merz, K. M., Jr.; Ferguson, D. M.; Sellmeyer, D. C.; Fox, T.; Caldwell, J. W.; Kollman, P. A. *J. Am. Chem. Soc.* **1995**, *117*, 5179.
(23) Barone, V.; Capecchi, G.; Brunel, Y.; Dheu Andries, M. L.; Subra, R. *J. Comput. Chem.* **1997**, *14*, 1720.
(24) Hyper Chem, *Release 4.5 for Windows*, Hypercube Inc.: Waterloo, Ontario, Canada, 1995.
(25) Cerius^2, *Release 3.0*, Molecular Simulations Inc.: San Diego, CA, 1997.
(26) Allinger, N. L. *J. Am. Chem. Soc.* **1977**, *99*, 8127 and subsequent versions e.g., MM2-87, MM2-89, MM2-91.
(27) (a) Rappé, A. K.; Casewit, C. J.; Colwell, K. S.; Goddard, W. A., III.; Skiff, W. M. *J. Am. Chem. Soc.* **1992**, *114*, 10024. (b) Rappé, A. K.; Colwell, K. S.; Casewit, C. J. *Inorg. Chem.* **1993**, *32*, 3438.
(28) Barone, V.; Bencini, A.; Benelli, C.; Fantucci, P.; Mattesini, M.; Totti, F., in preparation.
(29) (a) Barone, V. *Chem. Phys. Lett.* **1996**, *262*, 201. (b) Rega, N.; Cossi, M.; Barone, V. *J. Chem. Phys.* **1996**, *105*, 11060; *J. Am. Chem. Soc.* **1997**, *119*, 12962.
(30) Symons, M. C. R.; Pena-Nuñez, A. *J. Chem. Soc., Faraday Trans. 1*, **1985**, *81*, 2421.

also developed intermolecular parameters by fitting the structures and interaction energies for the adducts of a representative nitroxide radical with two water molecules obtained by DF computations.

The paper is organized as follows. After a short description of the computational details, two sections are devoted to the validation of the DFT approach for the study of structural and spectromagnetic properties of model nitroxides and to the development of MM parameters for the NO moiety. In the next sections, we report the essential details of three case studies: the singlet−triplet splitting of a large biradical, the calculation of the crystal structure of PROXYL, and the modifications induced by the solvent on the hyperfine parameters of rigid nitroxides.

Computational Details

All the quantum-mechanical computations are based on the unrestricted Kohn−Sham (UKS) approach to DF theory[31] as implemented in the GAUSSIAN-94 package.[32] On the basis of previous experience,[16,29] we have selected the B3LYP hybrid functional, which combines Hartree−Fock and Becke[33] exchange terms with the Lee−Yang−Parr correlation functional,[34] in the same ratios as those optimized by Becke for a similar (albeit not identical) functional.[35] The standard 6-31G* basis set[36] has been used for geometry optimizations, whereas interaction energies have been computed by the 6-311G** basis set[36] and magnetic properties by the purposely developed EPR-2 basis set.[16,17]

A particularly attractive model for the study of magnetic exchange interactions has been suggested by Noodleman and Case,[37] which is based on a broken spin and space symmetry single-determinant wave function for describing the low-spin state, accounting for a large part of the electron correlation. Next, a one-to-one correspondence is established between the energy of a Slater determinant built up with orbitals localized on different centers and bearing electrons with opposite spin and the energy of the microstate with $M_s = 0$ computed using the effective Heisenberg−Dirac-VanVleck (HDVV) spin Hamiltonian[38]

$$H = -2JS_1S_2 \tag{1}$$

This spin Hamiltonian is widely used to phenomenologically account[9] for magnetic exchange interactions, J being defined by

$$E(S) - E(S-1) = -2JS \tag{2}$$

where $E(S)$ represents the energy of a state with total spin S. J is known as the magnetic exchange coupling constant. For a dinuclear system of spin S_1 and S_2, the energy of the broken symmetry (BS) state is a weighted average of the energies of pure spin multiplets, and J can be obtained through the equation

$$-2\mathrm{J} = \frac{E(S_1 + S_2) - E(\mathrm{BS})}{2S_1S_2} \tag{3}$$

where E(BS) is the energy of the broken symmetry determinant. The term broken symmetry state refers to the fact that a localized solution of the spin states is usually obtained by using an electronic symmetry lower than the actual geometric symmetry. Equation 3 can be viewed as an effective recipe that allows one to compute J directly from the SCF calculation of two single determinants.[39]

Hyperfine splittings (hfs) of free radicals observed in ESR spectroscopy are determined by the electron spin density ρ_s at or near the position of any magnetic nucleus. In particular, the Fermi contact term of a nucleus N (the only one considered in the following) is given by[10]

$$a(N) = \frac{8}{3}\pi g_N g_e \mu_N \mu_e \rho_s(r_N) \tag{4}$$

where μ_N and g_N are the nuclear magneton and nuclear g factors, respectively. The term g_e is the g value for the electron, and μ_e is the Bohr magneton. In the present work a value of 2.0 is used for g_e.

Solvent effects have been evaluated by our recent implementation of the polarizable continuum model (PCM),[40] which is based on a self-consistent solution of the quantum mechanical problem of a molecule immersed in a polarizable continuum. The cavity created by the solute in the solvent is defined in terms of spheres centered on non-hydrogen atoms with radii optimized in a recent study (UAHF model).[41]

The molecular mechanics computations have been performed by the MM+[26] and UFF[27] force fields available in the Hyperchem and Cerius[2] packages,[24,25] respectively.

Results for the Training Set of Nitroxides

(a) B3LYP Computations. In Tables 1−4, the experimental geometries[42,43] of four of the radicals shown in Figure 1 are compared with the structures issuing from full optimizations at the B3LYP level. All the bond lengths calculated by the UB3LYP approach are close to their experimental counterparts. As shown in previous work,[44] reasonable results are also obtained at the HF level except for the NO bond length, which is very sensitive to basis set extension and to inclusion of correlation energy. NO bond lengths in the experimental range (1.26−1.29 Å) can be obtained only by introducing the electron

(31) Parr, R. G.; Yang, W. *Density Functional Theory of Atoms and Molecules*; Oxford University Press: New York, 1989.
(32) Frisch, M. J.; Trucks, G. W.; Schlegel, H. B.; W. Gill, P. M. W.; Johnson, B. G.; Robb, M. A.; Cheeseman, J. R.; Keith, T. A.; Petersson, G. A.; Montgomery, J. A.; Raghavachari, K.; Al-Laham, M. A.; Zakrewski, V. G.; Ortiz, J. V.; Foresman, J. B.; Cioslowski, J.; Stefanov, B. B.; Nanayakkara, A.; Challacombe, M.; Peng, C. Y.; Ayala, P. Y.; Chen, W.; Wong, M. W.; Andres, J. L.; Replogle, E. S.; Gomperts, R.; Martin, R. L.; Fox, D. J.; Binkley, J. S.; DeFrees, D. J.; Baker, J.; Stewart, J. P.; Head-Gordon, M.; Gonzalez, C.; Pople. J. A. *Gaussian 94 (Revision D.4)*, Gaussian Inc.: Pittsburgh, PA, 1996.
(33) Becke, A. D. *Phys. Rev. B* **1988**, *38*, 3098.
(34) Lee, C.; Yang, W.; Parr, R. G. *Phys. Rev. B* **1988**, *37*, 785.
(35) Becke, A. D. *J. Chem. Phys.* **1993**, *98*, 1372.
(36) Description of basis sets and standard computational models can be found in: Foresman, J. B.; Frisch, A. E. *Exploring Chemistry with Electronic Structure Methods*, 2nd ed.; Gaussian Inc., Pittsburgh, PA, 1996.
(37) Noodleman, L.; Case, D. *Adv. Inorg. Chem.* **1992**, *38*, 423.
(38) (a) Heisenberg, W. *Z. Phys.* **1928**, *49*, 619. (b) Dirac, P. A. M *Proc. R. Soc.* **1929**, *A123*, 714. (c) van Vleck, J. H. *The theory of Electric and Magnetic Susceptibility*; Oxford University Press: London, 1932.
(39) Bencini, A.; Totti, F.; Daul, C. A.; Doclo, K.; Fantucci, P.; Barone, V. *Inorg, Chem.* **1997**, *36*, 5022.
(40) (a) Cossi, M.; Barone, V.; Cammi, R.; Tomasi, J. *Chem. Phys. Lett.* **1996**, *255*, 327. (b) Barone, V.; Cossi, M.; Tomasi, J. *J. Comput. Chem.* **1998**, *19*, 407. (c) Cossi, M.; Barone, V. *J. Phys. Chem. A* **1998**, *102*, 1995.
(41) Barone, V.; Cossi, M.; Tomasi, J. *J. Chem. Phys.* **1997**, *107*, 3210.
(42) (a) Chion, B.; Lajzèrowicz, J.; Collet, A.; Jacques, J. *Acta Crystallogr.* **1976**, *B32*, 339. (b) Lajzèrowicz, J. *Acta Crystallogr.* **1968**, *B24*, 196.
(43) Andersen, B.; Andersen, P. *Acta Chem. Scand.* **1966**, *20*, 2718.
(44) (a) Barone, V.; Grand, A.; Minichino, C.; Subra, R. *J. Phys. Chem.* **1993**, *97*, 6355. (b) Komaromi, I.; Tronchet, J. M. *J. Phys. Chem.* **1995**, *99*, 10213. (c) Barone, V.; Grand, A.; Minichino, C.; Subra, R. *J. Phys. Chem.* **1993**, *97*, 6355.

Table 1. Geometrical Parameters (Distances in Å and Angles in Degrees) for the Dimethyl Nitroxide Radical (MNO)

	Exp	MM+	UFF	B3LYP
O(1)−N(2)	1.28	1.282	1.287	1.282
N(2)−C		1.476	1.458	1.463
O(1)−N(2)−C		118.4	120.1	119.4
C−N(2)−C	118.9	120.8	119.8	115.5

Table 2. Geometrical Parameters (Distances in Å and Angles in Degrees) for the Di(*tert*-butyl)aminoxyl Radical (TBNO)

	exp[a]	MM+	UFF	B3LYP
N(2)−O(1)	1.280 ± 0.020	1.284	1.295	1.287
N(2)−C(4)	1.512 ± 0.020	1.513	1.492	1.511
C(4)−C(5)	1.534 ± 0.020	1.550	1.620	1.545
C(4)−C(6)	1.534 ± 0.020	1.537	1.590	1.540
C(4)−C(7)	1.534 ± 0.020	1.538	1.595	1.540
C(3)−N(2)−C(4)	136 ± 3	127.0	125.0	127.9
C(5)−C(4)−C(7)	107 ± 2	113.5	112.7	110.9
C(6)−C(4)−C(7)	107 ± 2	108.2	106.4	108.6
C(5)−C(4)−C(6)	107 ± 2	107.0	106.2	107.8
τ	0.0	0.0	0.0	0.0
O(1)−N(2)−C(4)−C(5)	137 ± 2	135.2	137.3	138.3

[a] From ref 43.

Table 3. Geometrical Parameters (Distances in Å and Angles in Degrees) for the 2,2,5,5-Tetramethyl-3-hydroxypyrrolidine-1-oxyl Radical (PROXYL)

	exp[a]	MM+	UFF	B3LYP
N(1)−O(6)	*1.264*	*1.279*	*1.269*	*1.273*
N(1)−C(2)	*1.478*	*1.478*	*1.475*	*1.481*
N(1)−C(5)	*1.489*	*1.479*	*1.480*	*1.488*
C(5)−C(11)	1.531	1.535	1.529	1.524
C(5)−C(10)	1.525	1.536	1.520	1.536
C(2)−C(7)	1.542	1.536	1.536	1.543
C(2)−C(8)	1.518	1.536	1.504	1.533
C(5)−C(4)	1.521	1.539	1.515	1.544
C(2)−C(3)	1.524	1.538	1.517	1.530
C(4)−C(3)	1.531	1.536	1.524	1.556
C(3)−C(9)	1.399	1.402	1.403	1.418
O(6)−N(1)−C(2)	*122.0*	*122.1*	*122.7*	*123.6*
O(6)−N(1)−C(5)	*122.7*	*122.3*	*124.4*	*123.0*
C(5)−N(1)−C(2)	*115.3*	*115.8*	*113.0*	*113.3*
N(1)−C(5)−C(4)	101.6	102.5	103.6	103.4
N(1)−C(2)−C(3)	99.9	101.9	101.1	102.6
C(5)−C(4)−C(3)	104.8	103.8	103.4	104.7
C(2)−C(3)−C(4)	105.6	104.7	104.6	110.2
C(2)−C(3)−O(9)	111.7	111.7	111.6	114.5
N(1)−C(5)−C(11)	106.8	107.3	109.3	109.4
N(1)−C(2)−C(8)	109.9	106.9	108.0	113.3
N(1)−C(2)−C(7)	108.7	108.3	108.1	112.4
C(8)−C(2)−C(7)	111.8	112.4	109.3	109.3
N(1)−C(5)−C(10)	109.5	107.6	109.6	109.4
C(10)−C(5)−C(11)	110.2	112.5	113.5	113.3
τ	*0.0*	*0.0*	*2.2*	*3.0*
O(6)−N(1)−C(5)−C(4)	175.6	170.2	176.0	173.9
O(6)−N(1)−C(2)−C(3)	162.7	168.9	161.0	164.9
N(1)−C(5)−C(4)−C(3)	24.6	26.7	25.9	22.6
C(5)−C(4)−C(3)−C(2)	−36.6	−34.0	−38.3	−34.2
N(1)−C(2)−C(3)−C(4)	31.6	27.3	33.6	31.5
N(1)−C(2)−C(3)−O(9)	154.8	147.4	152.6	154.9
O(6)−N(1)−C(2)−C(8)	44.2	50.1	42.6	44.8
O(6)−N(1)−C(2)−C(7)	−78.4	−71.3	−77.5	−75.6
O(6)−N(1)−C(5)−C(10)	54.0	50.7	54.6	52.9
O(6)−N(1)−C(5)−C(11)	−65.3	−71.1	−63.7	−66.6

[a] From ref 42a.

correlation at least at the second order of perturbative treatment (MP2) or by using gradient-corrected density functionals including a fraction of the HF exchange (B3LYP). Very similar N−O bond lengths have been observed for all radicals except PROXYL, which is characterized by a more extensive π delocalization. Since the singly occupied molecular orbital

Table 4. Geometrical Parameters (Distances in Å and Angles in Degrees) for the (2,2,6,6-Tetramethyl-4-piperidinol-1-oxyl) Radical (TANOL)

	exp[a]	MM+	UFF	B3LYP
N−O(1)	*1.291*	*1.283*	*1.296*	*1.285*
N−C(3)	*1.498*	*1.496*	*1.511*	*1.503*
C(3)−C(2)	1.526	1.538	1.529	1.542
C(2)−C(1)	1.517	1.526	1.517	1.528
C(1)−O(2)	1.422	1.406	1.400	1.426
O(2)−H	0.895	0.942	0.901	0.971
C(3)−C(4)	1.540	1.540	1.526	1.544
C(3)−C(5)	1.534	1.545	1.523	1.537
O(1)−N−C(3)	*116.2*	*116.8*	*116.5*	*115.6*
C(3)−N−C(3)	*125.4*	*124.6*	*126.2*	*124.7*
N−C(3)−C(4)	108.4	108.3	108.5	109.2
N−C(3)−C(5)	107.7	107.5	106.6	107.1
C(5)−C(3)−C(4)	110.5	109.3	110.4	109.2
N−C(3)−C(2)	110.1	109.9	109.6	110.1
C(3)−C(2)−C(1)	113.1	113.0	114.2	114.1
C(2)−C(1)−O(2)	112.3	108.9	112.1	111.7
C(1)−O(2)−H	104.3	107.6	105.4	107.4
C(2)−C(1)−C(2)	108.3	107.7	108.4	109.1
τ	*15.8*	*16.6*	*14.3*	*13.6*
O(1)−N−C(3)−C(2)	−167.5	−159.0	−166.2	−169.7
O(1)−N−C(3)−C(4)	−71.1	−77.1	−72.4	−67.4
O(1)−N−C(3)−C(5)	48.5	40.8	48.3	50.7
N−C(3)−C(2)−C(1)	44.6	46.4	43.0	44.9
C(3)−C(2)−C(1)−O(2)	173.3	178.4	175.2	177.3
C(2)−C(1)−O(2)−H	61.1	70.5	60.3	61.2

[a] From ref 42b.

(SOMO) is antibonding between N and O, reduction of the electron population in this region strengthens the N−O bond, which becomes significantly shorter. The bond angles obtained by B3LYP/6-31G* calculations show an error of about 2% with respect to experimental values. The C−N−C angle is larger than the O−N−C one (125 vs 116°) in all of the radicals except PROXYL (C−N−C = 113.3°, O−N−C = 123.6°). This inversion is due to the constraint that none of the angles of the five-membered ring (including the C−N−C angle) can deviate too much from the value of 108° characterizing a regular pentagon. Also, the out-of-plane angles calculated at the B3LYP/6-31G* level are very close to experimental values. Furthermore, the very small inversion barriers indicate that nitroxides are in most cases quasi-planar molecules (i.e., the ground vibrational level is above or very close to the inversion barrier) so that the orbital containing the odd electron has an almost pure π^* character.[45] The structure of the resulting radical, which has a formal NO bond order of 1.5, is either planar or bent, depending on whether stabilization from partial π bonding is sufficient to retain a pure sp^2 hybridization of the nitrogen. The competition between π bonding and the intrinsic preference of nitrogen for a pyramidal environment (i.e., sp^3 hybridization) explains the extremely flat potential energy surface for the out-of-plane motion and the occurrence of both planar and pyramidal structures depending on actual molecular topologies.[42]

It is well-known that one of the most serious drawbacks of unrestricted computations on open-shell species is that the resulting wave function is not an eigenstate of the S^2 operator. Although the DF approach does not use, in principle, any well-defined wave function, the spin density is evaluated using a reference set of KS orbitals. Under such circumstances, a reliable estimation of the expectation value of S^2 can be computed using these orbitals. It is then remarkable that spin contamination is very low in the UKS approach for all the open-

(45) Griffith, O. H.; Cornell, D. W.; McConnell, H. M. *J. Chem. Phys.* **1965**, *43*, 2909.

Table 5. Geometrical Parameters (Distances in Å, Angles in Degrees) and Isotropic hfs (a(X) in G) for the Dihydronitroxide Radical Obtained by Different Methods

	UHF	ROHF	UMP2	UQCISD	B3LYP	exp[a]
r(NO)	1.262	1.273	1.257	1.278	1.277	1.280
r(NH)	0.996	1.005	1.008	1.016	1.015	1.01
HNH	118.4	115.5	119.3	119.0	119.0	122.7
τ	26.7	36.5	0.0	16.90	16.6	0(?)
ΔE	1.10	3.6	0.0	0.2	0.2	
a(^{14}N)	13.6	12.8	13.4	10.1	7.6	9.7
a(H)	−16.8	−5.2	−14.8	−11.0	−10.9	−10.5

[a] From ref 46.

Table 6. Geometrical Parameters (Distances in Å, Angles in Degrees), Isotropic hfs (a(X) in G) and Atomic Spin Populations (ρ_s(X)) of Nitronyl Nitroxide Radical Obtained by Different Methods

	exp (R6 = CH_3)[a]	B3LYP (R6 = H)	MM+ (R6 = H)
N(1)−C(2)	1.335	1.345	1.344
N(1)−O	1.290	1.269	1.278
N(1)−C(5)	1.488	1.491	1.483
C(4)−C(5)	1.540	1.538	1.545
N−C−N	107.9	112.4	112.5
C−N−C	112.1	110.3	110.3
C−N−O	125.0	127.9	127.9
a(N)	±7.26	4.92 (7.12)[b]	
a(C2)	±12.36	−15.07	
a(C4)	±6.00	−4.15	
ρ_s(N)	0.257	0.284	
ρ_s(O)	0.283	0.342	
ρ_s(C2)	−0.090	−0.268	

[a] From ref 50. [b] Adding the difference between QCISD[T] and B3LYP values for the planar structure of H_2NO.

shell systems considered in the present study, whereas much higher spin contaminations are obtained by the UHF approach.

Let us now consider the suitability of the B3LYP method for computing reliable spectromagnetic properties. The most significant physicochemical observables of the simplest nitroxide, H_2NO, obtained by different methods are shown in Table 5. Taking the UQCISD[T] results[44c] as a reference rather than experimental values[46] (which involve some structural assumption and significant vibrational averaging), it is quite apparent that only the B3LYP approach provides reliable results. The only departure from the reference values concerns a slight underestimation of the isotropic hfs of nitrogen. However, general trends are correctly reproduced for this quantity also.[16,29] This is confirmed by the results obtained for the simplest nitronyl nitroxide sketched in Figure 1 (hereafter NITNO), which are shown in Table 6. Once again structural data are in fair agreement with experiment,[47] and this is also the case for all hfs's.[48] Furthermore, adding to the B3LYP value computed for *a(N)* (4.92 G) the difference between QCISD[T] and B3LYP isotropic hfs's for the planar structure of H_2NO (2.20 G) leads to a value (7.12 G) in remarkable agreement with experiment (7.26 G). Note that conventional HF and post-HF approaches are significantly less successful in this connection.[49] Therefore, we suggest that accurate isotropic hfs's for nitrogen atoms in nitroxides can be obtained by increasing the B3LYP results by a constant amount, 2.20 G. When needed, vibrational averaging and solvent effects computed at the B3LYP level can be added to the static in vacuo results.

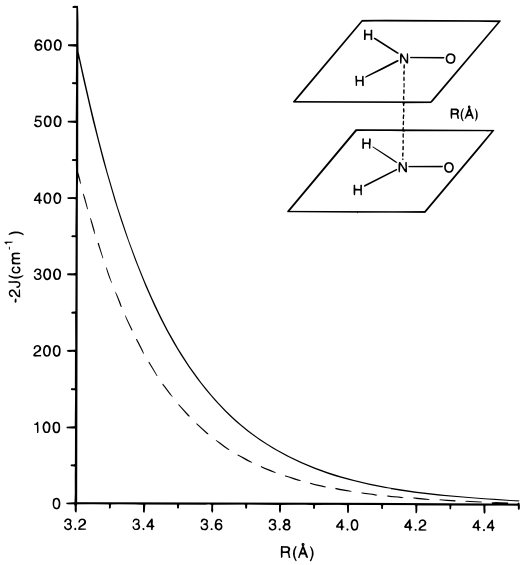

Figure 2. Magnetic coupling, $2J$ (cm^{-1}), computed by BS/B3LYP (—) and dedicated CI (- - -) for the dihydronitroxide dimer using the 6-31G* basis set.

Atomic spin populations (ASPs) for the nitronyl nitroxide radical have been obtained by single-crystal polarized neutron diffraction on a derived nitrophenyl.[50] The values reported in Table 6 indicate that most of the spin density is located on N and O atoms. B3LYP ASPs are generally close to experimental values, except that of the C atom, probably due to some residual overestimation of spin polarization effects.[51] Note, however, that this effect is attenuated when a phenyl is bonded to this atom.[51] Moreover the spin repartition between different atoms obtained at the B3LYP level is at least in qualitative agreement with experiment. This finding is quite satisfactory, taking into account the assumptions made both in quantum mechanical computations and in the elaboration of experimental data. Once again, significantly poorer results are obtained by conventional HF and post-HF models.[50,51]

Together with their intrinsic interest, the above results pave the route for reliable computations of magnetic interactions in organic magnets. Of course, the other important ingredient for this task is the correct behavior of the computed magnetic coupling as a function of the distance and/or orientation between the interacting units. This aspect has been verified by considering the interaction between two H_2NO radicals in the orientation shown in Figure 2, which leads to an antiferromagnetic system. We have considered in particular the region in which the absolute value of the magnetic coupling is in the physically significant range of 0−500 cm^{-1} by using for purposes of reference the very accurate dedicated CI approach[52] implemented in a locally modified version of the HONDO/CIPSI program.[53] The results shown in Figure 2 indicate that the BS/B3LYP model allows a semiquantitative evaluation for a wide

(46) Mikami, H.; Saito, S.; Yamamoto, S. *J. Chem. Phys.* **1991**, *94*, 3415.

(47) (a) Barone V.; Grand, A.; Luneau, D.; Rey, P.; Minichino, C.; Subra, R.; *New. J. Chem.* **1993**, 17, 1587. (b) Grand, A.; Rey, P.; Subra, R.; Barone, V.; Minichino, C. *J. Phys. Chem.* **1991**, *95*, 9238.

(48) (a) Boocock, D. G. B.; Darcy, R.; Ullman, E. F. *J. Am. Chem. Soc.* **1968**, *90*, 5945. Gough, T. E.; Purzic, R. *J. Magn. Reson.* **1976**, *23*, 31.

(49) Cogne, A.; Grand, A.; Rey, P.; Subra, R. *J. Am. Chem. Soc.* **1989**, *111*, 3230.

(50) Zheludev, A.; Barone V.; Boumet, M.; Delley, B.; Grand, A.; Ressouche, E.; Rey, P.; Subra, R.; Schweizer, J. *J. Am. Chem. Soc.* **1994**, *116*, 2019.

(51) Barone, V.; Bencini, A.; di Matteo, A. *J. Am. Chem. Soc.* **1997**, *119*, 10831.

(52) Castell, O.; Miralles, J.; Caballol, R.; Malrieu, J. P. *Chem. Phys.* **1994**, *179*, 377.

(53) Daudey, J. P.; Malrieu, J. P.; Maynau, D.; Pellissier, M.; Spiegalman, F.; Caballol, R.; Evangelisti, S.; Illas, F.; Rubio, J. PSH−CIPSI. program package.

rage of magnetic couplings at a fraction of the cost of the dedicated CI approach. This confirms the conclusions reached in a previous paper devoted to intramolecular magnetic interactions.[51]

By summarizing, all the results reported in this section, together with several other unpublished computations, strongly suggest that reliable spectromagnetic properties can be computed by the B3LYP model provided that accurate geometrical structures are available. Although geometry optimizations are feasible at the B3LYP level for quite large systems, it would be preferable to develop a cheaper procedure based on the molecular mechanics approach in order to concentrate the computational resources to accurate single point computations of energies and physicochemical observables. This is the topic of the next section.

(b) Optimization of MM Parameters. There are two characteristics of the NO moiety that need special consideration for a correct development of the force field. The first aspect is that, as discussed in the Introduction, the unpaired spin of nonconjugated nitroxides is well localized on the diatomic functional NO moiety, so that addition of just two new atom types to current force fields should be sufficient to account for the particular nature of the bond. The second aspect is that both the preference for a planar or pyramidal enviroment of the N atom and the partitioning of the spin density between the N and O atoms are strongly dependent on the nature of its substituents.[44] This effect is certainly responsible for the difficulties encountered in the experimental determination of geometrical parameters and calls for a careful optimization of the out-of-plane bendings and torsions of the NO moiety. Unfortunately, this point has been completely overlooked in a recent parametrization of the MM2 force field for nitroxide radicals,[54] so that we have undertaken a completely new parametrization.

In most MM methods the total energy can be partitioned as follows:[26,27]

$$E_{\text{total}} = \sum_{\text{bonds}} K_r(r - r_0)^2 + \sum_{\text{angles}} K_\theta(\theta - \theta_0)^2 + \sum_{\text{dihedral}} K_\varphi(1 + \cos(n\varphi - \varphi_0)) + E_{\text{impr}} + E_{\text{elect}} + \sum_{ij} \epsilon_{ij} f(R^*_{ij}/R_{ij}) \quad (5)$$

We have retained the parameters of the original force fields except for interactions involving the new NR and OR atom types, whose parameters are given in Table 7. Bond stretchings, angle bendings, and regular torsions are described in a similar way in both the force fields used in this work. Higher order terms, i.e., cubic stretching and sextic angle bending for the MM+ force field, are not reported since we have retained their standard values.

Starting from standard values for N and O atoms, stretching and bending parameters have been refined by trial and error until a good agreement with B3LYP results was reached. Although harmonic frequencies are not a specific topic of the present work, it is gratifying that our parameters lead to a good agreement between the computed (1496 and 1384 cm^{-1}) and experimental (1440 and 1373 cm^{-1}) N−O stretching frequencies for PROXYL and TANOL, respectively.

A deeper attention has been paid to improper and regular torsional parameters, since a correct description of the out-of-plane bending of the NO moiety is one of the main objectives of this work. As already mentioned, Sakakibara et al.[54] have recently extended the MM2 force field to nitroxide radicals without taking into account the particular flexibility of the NO moiety. As a consequence, their parameters lead, contrary to the experimental data, to a pyramidal structure of the TBNO radical. The electronegativity of groups directly bonded to the NO moiety plays an important role in tuning the value of the out-of-plane angle τ. However, the differences between MNO (pyramidal) and TBNO (planar) on one hand and PROXYL (planar) and TANOL (pyramidal) on the other hand have clearly another origin. The out-of-plane angle (τ) of the NO moiety is almost insensitive to the C−N bond length, but it regularly increases, decreasing the C−N−C (β) bond angle, the relationship being linear in the range $110° < \beta < 130°$. Although this finding could explain the differences between MNO ($\beta = 120°$, $\tau = 30°$) and TBNO ($\beta = 135°$, $\tau = 0°$), it does not offer a rationalization for the planarity of nitroxides involved in five-membered rings ($\beta = 115°$). In an attempt to better elucidate this point, we also consider the influence of the C−N−C−C (ϕ or τ) torsional angles on the out-of-plane motion. Komaromi and Tronchet[44b] have shown that a relationship can be found between τ and the out-of-plane angle of the NO moiety: whenever ϕ or τ are close to $(60 + 120k)°$ ($k = 0$, 1, or 2), the out-of-plane angle is larger than 20°. This situation is found for freely rotating groups (e.g., MNO) or when these values of ϕ or τ are imposed by the presence of cyclic structures (e.g., in the chair form of TANOL). Values of ϕ or τ close to $(120k)°$ ($k = 0$,1, 2) are, instead, found when five-membered rings are

Table 7. Optimized MM Parameters Involving NR, OR, and Lp Species[a]

bond stretching	R_0 (Å)	K_r (kcal mol^{-1} Å^{-2})
NR−OR	1.279	337.0
C−NR	1.470	450.1
CA−NR	1.345	500.0
Lp−OR	0.50	325.0
angle bendings	θ_0 (deg)	K_θ (kcal mol^{-1} rad^{-2})
NR−C−C	105.6	80.00
C−NR−C	120.0	46.56
OR−NR−C	119.3	80.23
H−C−NR	109.5	50.00
NR−CA-NR	122.0	50.40
CA−NR−OR	124.0	50.40
CA−NR−C	122.0	25.20
Lp−OR−Lp	120.0	80.00
Lp−OR−NR	120.0	80.00
improper torsions	ϕ_0 (deg)	K_ϕ (kcal mol^{-1} rad^{-2})
NR−C−C−OR[b]	0.0	3.95
NR−Or[c]	0.0	1.20
NR−C[c]	0.0	1.20
OR-Lp[c]	0.0	10.00
regular torsions	τ_0 (deg)	$V_3/2$ (kcal mol^{-1})
NR−C−C−*	0.0	0.222
−NR−C−	0.0	0.333
−NR−CA−[d]	0.0	6.250
*−NR−OR−Lp[c,d]	0.0	1.000
nonbond interact (VdW)	R^*_{ii} (Å)[e]	ϵ_{ii} (kcal mol^{-1})[f]
NR	3.66	0.0690
OR	3.48	0.0598
Lp[c]	2.00	0.0600
hydrogen bond[b]	R^*_{ij} (Å)	ϵ_{ij} (kcal mol^{-1})
OR−O3	2.82	0.0300

[a] See text for further details. [b] UFF. [c] MM+. [d] $V_2/2$ in place of $V_3/2$. [e] $R^*_{ij} = (R^*_i + R^*_j)/2$. [f] $\epsilon_{ij} = (\epsilon_{ii}\epsilon_{jj})^{1/2}$.

(54) Sakakibara, K.; Kawamura, H.; Nagata, T.; Ren, J.; Hirota, M.; Shimazaki, K.; Cheman, T. *Bull. Chem. Soc. Jpn.* **1994**, *67*, 2768.

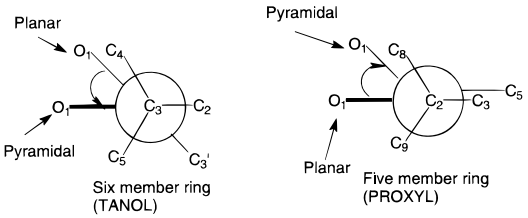

Figure 3. Torsional angles around the NO moiety.

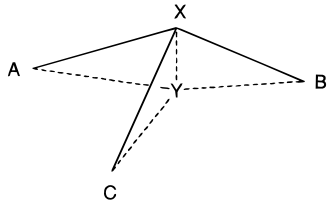

Figure 4. Definition of improper torsions in different force fields.

present (e.g., in PROXYL) and lead to out-of-plane angles in the range $0° < \tau < 5°$.

All these trends can be explained in terms of the preference for staggered dispositions of the groups bonded to R−C−N(R)−R (R or O(R)). In the case of molecular systems with six- or five-membered rings, the torsional angles are fixed (see Figure 3). In the six-membered ring, a planar disposition of the O1 atom induces an eclipsed conformation between the O1 and C4 atoms whereas a staggered conformation can be reached upon pyramidalization of the NO moiety. On the other hand, for nitroxides involving a five-membered ring, a pyramidal conformation of the NO group leads to an eclipsed conformation between the O1 and C8 atoms, whereas a planar conformation allows a staggered conformation between these atoms (see Figure 3).

For both five- and six-membered rings the C−C−N(R)−C torsional angles are fixed by the topology of the system and they do not need any particular torsional potential, while for the C−C−N(R)−O(R) torsional angle, a new parametrization with minima at $(60 + 120k)°$ ($k = 0, 1, 2$) must be introduced. For systems such as MNO and TBNO in which there is a free rotation of CH_3 and $C(CH_3)_3$ groups, the correct staggered conformations can be obtained only using torsional potentials for C−C−N(R)−O(R) and C−C−N(R)−X (X = C, H) with minima at $(60 + 120k)$ ($k = 0, 1, 2$): we selected a minimalist approach in which only a generic 3-fold Fourier component (V_3) is introduced for all rotations around the C−N(R) bond (see Table 7).

The term E_{impr} appearing in eq 5 accounts for the out-of-plane bendings of the NO group and it is treated differently in MM+ and UFF. In particular, the UFF force field employs the expression

$$E_{\text{impr}} = \sum_{\text{torsion}} K_\tau(\tau - \tau_0)^2 \qquad (6)$$

where the out-of-plane displacement of a X−B bond is defined in terms of the angle τ between the X−B bond and the AXC plane (see Figure 4).

In the case of the MM+ force field, the out-of-plane bending around a three-coordinated atom (X) is defined in terms of the projection of X onto the ABC plane (Y). Thus, in addition to the three angles AXC, AXB, and BXC, bending contributions are also calculated for the angles XAY, XBY, and XCY. Deformations of these latter three angles are governed by harmonic potentials with minima for vanishing angles and special bending constants. Three new types of improper torsions are sufficient to describe all the situations involving the NO moiety (see Table 7).

Electrostatic interactions (E_{elect} in eq 5) have been described either by the bond dipoles optimized by Sakakibara and coworkers[54] for N−O and C−N bonds (only in MM+), or by atomic point charges using a unitary (i.e., vacuum) dielectric constant (both in MM+ and UFF). The use of either bond dipoles or atomic charges affords comparable structures for the isolated species, while only atomic charges give satisfactory results in condensed phases. The standard electronegativity equalization procedure has been used to generate UFF charges,[22] whereas for MM+ we have resorted to the powerful restrained electrostatic potential (RESP) procedure recently introduced by Bayly et al.[55] This model is based on a least-squares fitting of HF/6-31G** electrostatic potentials, but with the addition of hyperbolic restraints on the charges of non-hydrogen atoms. These restraints allow one to reduce the charges on atoms (e.g., buried carbons) that are poorly defined by the electrostatic potential. Furthermore, equivalent charges are imposed to geminal hydrogens. This choice, together with its formal elegance and generality, allows direct transfer of all the atomic charges of biological fragments available in the AMBER/95 database to the new force field.[22] Inspection of the charges derived by this procedure, together with several test computations, convinced us that quantum mechanical computations for large systems can be completely avoided without significant loss of precision by introducing the following general rules: (1) Hydrogen atoms have fixed charges of 0.06, 0.14, 0.28, 0.43, and 0.43 au when bound to sp^3 carbons, sp^2 carbons, amidic nitrogens, aminic nitrogens, and alcoholic oxygens, respectively. (2) Etheric and hydroxyl oxygens have charges of −0.35 and −0.65 au, respectively. (3) Amidic and aminic nitrogens have charges of −0.42 and −0.92 au, respectively. (4) The N and O atoms of the nitroxide moiety have charges of 0.17 and −0.31 au, respectively. When explicit lone pairs are employed for the nitroxide oxygen (vide infra) each lone pair has a charge of −0.24 au and the oxygen charge becomes 0.17 au. (5) Each substituent of the NO moiety has a total charge of 0.07 au. (6) Methyl, methylene, CH_2X, and CHX ($X \neq sp^3$ C) groups not directly bound to heteroatoms are neutral.

The charges of all the systems considered in the present study can be obtained by the above rules and are given in Figure 1. In other cases, it is generally sufficient to transfer the lacking charges from similar compounds available in the AMBER/95 database or to perform a limited number of additional quantum mechanical computations for small systems followed by some manual adjustment to enforce the above rules and the electroneutrality condition.

The last term in eq 5 represents intra- and intermolecular interactions between nonbonded atoms as well as hydrogen-bonding interactions more relevant for condensed phases. They are a function of the van der Waals radii, R^*, and of the well depths ϵ that determine how easily two atoms of types i and j can approach each other. The VdW interactions are represented in the UFF by a (12−6) Lennard-Jones potential, whereas in MM+ the repulsive term has an exponential form. However, conversion between the two forms is straightforward, so that we could develop a common set of parameters. For the hydrogen bond interactions used to model the structure of nitroxides in the solid state by UFF a specific (12−10) potential was applied. The VdW parameters of OR and NR were initially set equal to those of the carbonyl oxygen and sp^2 nitrogen

(55) Bayly, C.; Cieplak, P.; Cornell, W.; Kollman, P. A. *J. Phys. Chem.* **1993**, *97*, 10269.

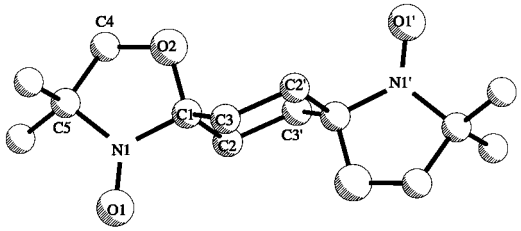

Figure 5. Structure and atom numbering of 1,4,bis(4,4-dimethyloxazolidine-*N*-oxyl) cyclohexane (OXYL).

already available in standard MM+ and UFF force fields. They were next optimized by minimizing the root-mean-square deviations ($rmsd_{cell}$) of crystal cells. This procedure was applied iteratively until a common set of parameters was achieved, describing correctly all the analyzed structures.

The geometries of the training set of nitroxides optimized with the final set of parameters are compared in Tables 1−4 to the experimental and B3LYP geometries. All the MM calculations reproduce correctly the geometrical parameters of the radicals contained in the training set. The N−O bonds are well reproduced for TBNO, TANOL, and MNO with a harmonic potential, whereas the shortening observed in the 3-hydroxy-PROXYL radical is reproduced only using a Morse stretching potential. The bond angles of the N−O moiety (shown in italics in the tables) are close to experimental data. The quite good agreement obtained for the other valence angles points out the reliability of the underlying force field.

As a last point, we have considered nitronyl nitroxides, which contain an sp^2 carbon atom. Using default MM+ parameters for this atom type (CA), we needed only to optimize the CA−NR stretching, the CA−NR−OR, NR−CA−NR and NR−CA−C bendings, and the OR−NR−CA−C torsion. The parameters reported in Table 7 were obtained by a few trial and error refinements, and Table 6 shows that they lead to a very accurate geometrical structure. As a consequence, all the nitroxide and nitronyl−nitroxide systems can be treated by our modified force fields.

Case Studies

(a) Organic Magnets. The interaction between magnetic centers is governed by two main factors: the exchange energy between electrons of equal spin, which favors a parallel spin alignment between adjacent centers, and the overlap between the magnetic orbitals, which favors an antiparallel spin alignment. Quantitative calculation of magnetic exchange interactions requires an accurate description of the multiplet structure of the molecule for the ground and the lowest excited states. We have recently shown that the BS/B3LYP approach provides values in close agreement with the experiment for a biradical nitroxide system.[51] However, the exchange coupling constant is strongly dependent on the geometrical parameters of the system and especially on the distance and relative orientation of the NO moieties. Thus, accurate geometries, as close as possible to experimental ones, are mandatory for reliable computations.

The 1,4-bis(4′,4′-dimethyloxazolidine-*N*-oxyl)cyclohexane[56] (OXYL) is a large diradical system (Figure 5) characterized, according to magnetization and ESR studies, by a singlet ground state with a small exchange interaction[57] ($2J = -29$ cm^{-1}).

Table 8. Geometrical Parameters (Distances in Å and Angles in Degrees) for 1,4-Bis(4,4-dimethyloxazolidine-*N*-oxyl)cyclohexane (OXYL)

geom param	exp[a]	MM+
C1−N1	1.511	1.486
C1−O2	1.421	1.422
C1−C2	1.561	1.545
C1−C3	1.532	1.531
N1−O1	1.252	1.282
N1−C5	1.523	1.487
O2−C4	1.354	1.421
C5−C4	1.551	1.542
C3−C2′	1.552	1.543
O1−O1′	*7.001*	*6.955*
N1−N1′	*5.752*	*5.722*
C1−C3−C2	109.0	111.1
C1−C2−C3	111.0	112.1
C2−C1−C3	113.0	112.0
O2−C1−N1	*103.0*	*104.3*
O2−C1−C3	113.0	110.9
C1−N1−O1	124.0	123.6
C1−N1−C5	109.0	111.6
C5−N1−O1	126.0	124.7
C1−O2−C4	114.0	108.1
O2−C4−C5	107.0	108.7
C4−C5−N1	101.0	99.8
C5−N1−C1−O2	−7.7	−10.8
C5−C4−O2−C1	−23.8	−29.4
C4−O2−C1−N1	19.9	24.3
O2−C4−C5−N1	16.3	20.9
C4−C5−N1−C1	−4.7	−5.8

[a] From ref 56.

The point charges of OXYL shown in Figure 1 were obtained by the procedure described in Optimization of MM Parameters. All the geometrical parameters obtained by MM+ calculations shown in Table 8 are very close to experimental values. It is particularly significant that the structure of the NO moieties and the distances between them (indicated in italics in Table 8) are in good agreement with the experimental values. The exchange coupling constant has been computed with the BS approach at the B3LYP/6-31G* level using the experimental geometry and the structures optimized at the B3LYP[58] and MM+ levels. All the values are close and all indicate, in agreement with experiment ($2J = -29$ cm^{-1}),[57] that the system is weakly antiferromagnetic ($2J = -29$, -24, and -26 cm^{-1} using experimental, B3LYP, and MM+ structures, respectively).

(b) Solid State. To verify whether the parameters used to model the molecules in the gas phase can be used for reproducing the structures of nitroxide radicals engaged in a crystalline environment, we have extended the molecular force field to include intermolecular interactions. With respect to gas-phase optimizations, a correct reproduction of crystal structures requires a proper account of periodic boundary conditions and of intermolecular noncovalent interactions. While electrostatic and VdW interactions have been taken explicitly into account in the parametrization of the NR and OR atom types, the description of hydrogen bond interactions between the hydroxide and nitroxide moieties requires the introduction of new parameters for the donor(O3)/acceptor(OR) couple, O3 being the standard atom type used to describe the sp^3 oxygen atom in the OH group.

The VdW and hydrogen bond parameters have been optimized to reproduce the packing of selected nitroxide radicals in the solid state, as detailed elsewhere.[28] The parameters for the O3/OR couple and for the NR and OR atom types differ significantly from the standard UFF parameters, while for C

(56) Gleason, W. B. *Acta Crystallogr.* **1973**, *B29*, 2959.

(57) (a) Michon, P.; Rassat, A. *J. Am. Chem. Soc.* **1975**, *97*, 696. (b) Gambarelli, S.; Jaouen, D.; Rassat, A.; Brunel, L. C.; Chachaty, C. *J. Phys. Chem.* **1996**, *100*, 9605.

(58) Barone, V.; di Matteo, A.; Illas, F.; Mele, F., to be published.

Table 9. Comparison between Cell Parameters of PROXYL (Distances in Å, Angles in Degrees) Computed by the UFF Method and Experimental Values

	exp[a]	UFF
a	9.953	9.945
b	6.678	6.665
c	13.940	13.961
α	90.00	89.99
β	90.00	89.95
γ	90.00	89.94
$rmsd_{cell}$		0.081

[a] From ref 42a.

Table 10. Solvent Shifts of Isotropic hfs's (G) with Respect to Their Values in *n*-Hexane for the 4-Amino-2,2,6,6-tetramethylpiperidy1-yloxy Radical (TANINE)

	PCM	adduct	adduct + PCM	exp[a]
N	0.96	1.27	1.82	1.77
C	−0.13	−0.11	−0.17	

[a] From ref 61.

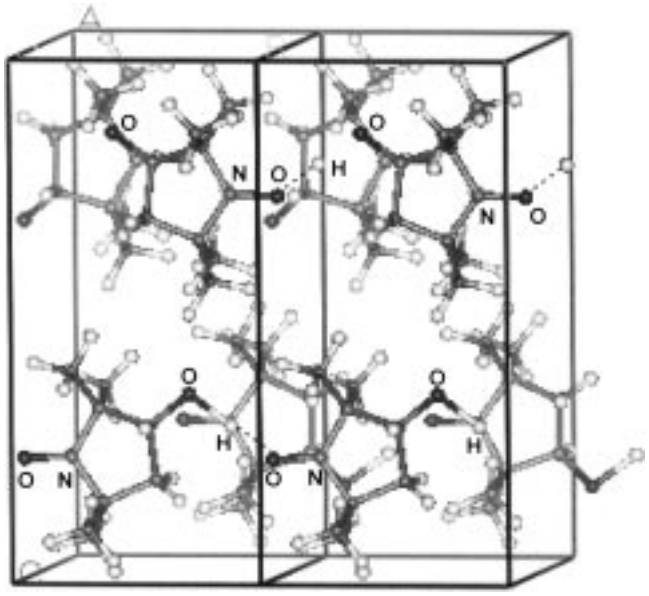

Figure 6. Schematic drawing of the two elementary cells of PROXYL ($Z = 4$) calculated with UFF. Hydrogen bonds are represented by dashed lines.

and H atom types, standard UFF values can be employed without any significant loss of precision. This is due to the prevalent localization of the unpaired spin density on the N−O site. The best-fit parameters are reported in Table 7. As an example of possible applications, we report in Table 3 the intramolecular parameters of the PROXYL radical and in Table 9 the corresponding cell parameters. A view of the unit cell of the radical, which contains four asymmetric molecular units, is shown in Figure 6. All the geometrical parameters are in close agreement with experiment, and in particular, an overall $rmsd_{cell} = 0.081$ is obtained on the cell parameters. This shows that we have at our disposal a very powerful tool also for studies in the solid state.

(c) Solution Properties. Our third application concerns the structures and magnetic properties of nitroxide radicals in aqueous solution. From an experimental point of view, spectroscopic observations unequivocally show that two water molecules are strongly and specifically bound to the nitroxide oxygen.[30] A reliable description of these hydrogen bond interactions is, therefore, mandatory. To this end, we have reparametrized the oxygen and hydrogen atoms of water in the MM+ force field with reference to the water dimer, which is experimentally well characterized. As a matter of fact, the standard MM+ parameters give quite poor results, whereas a simple modification of VdW parameters and net atomic charges (see Table 7) leads to results in good agreement with experiment and refined quantum mechanical computations. In particular, the O−O distance obtained by the modified MM+ parameters (3.01 Å) is only slightly longer than the accepted experimental value (2.95 Å) and the OH bond length for the atom involved in the hydrogen bridge (0.956 Å) is in fair agreement with the B3LYP value (0.973 Å). Also, the interaction energy computed at the MM+ level (5.84 kcal/mol) is in good agreement with experiment (5.44 kcal/mol) and with quantum mechanical computations (5.76 kcal/mol at the B3LYP/6-311G** level using the MM+ geometry).

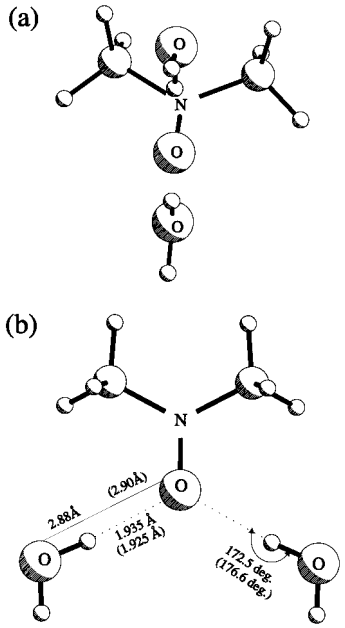

Figure 7. Optimized structures of the $H_2NO + 2H_2O$ adduct: (a) MM+ with atom centered charges; (b) comparison between MM+ with explicit lone pairs and B3LYP (in parenthesis).

We then performed several MM+ geometry optimizations in order to locate the absolute energy minimum for the model system $MNO + 2H_2O$. The most stable structure (Figure 7a) is quite unusual since the two water molecules reside on opposite sides of the mean molecular plane; i.e., they are perpendicular to the oxygen lone pairs. Geometry optimization at the B3LYP/6-311G** level leads to the much more reasonable structure shown in Figure 7b in which the water molecules lie in the molecular plane approximately along the directions of the oxygen lone pairs. The MM+ result is, however, quite reasonable, assuming a spherical electron distribution around the nitroxide oxygen. Under such circumstances, the water molecules prefer an orientation that minimizes steric repulsions with further substituents of the NO moiety; i.e., they avoid the mean molecular plane. The only way to obtain a reasonable structure at the MM+ level is to explicitly define lone pairs for the nitroxide oxygen. Although their specific parameters are not very critical, the best fitting of the B3LYP structure and energetics is obtained by the set given in Table 7. The intermolecular parameters are very similar by MM+ and B3LYP calculations (see Figure 7b) and the MM+ interaction energy (−10.7 kcal/mol) is close to the B3LYP/6-311G** result

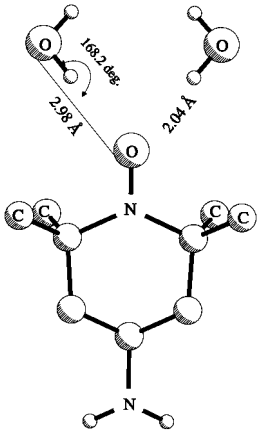

Figure 8. Structure of the adduct of 4-amino-2,2,6,6-tetramethylpiperidyl-1-yloxy radical (TANINE) with two water molecules optimized at the MM+ level with explicit lone pairs.

corrected for the basis set superposition error (BSSE) by the procedure introduced by Boys and Bernardi[59] (−10.4 kcal/mol).

It is gratifying that very similar parameters were recently obtained for the lone pairs of carbonyl oxygen in the AMBER force field.[60] Moreover, the intramolecular parameters of nitroxide radicals are only negligibly affected by the introduction of explicit lone pairs. Note that UFF computations in the solid state employ specific 10−12 interactions to describe hydrogen bonds, so that the force fields for solid and liquid phases are not strictly comparable. However, some test computations suggest that the same explicit lone pairs added to the MM+ force field could improve UFF results too, avoiding the use of specific H-bond parameters. Work is in progress to further verify this aspect.[28]

Using the parametrization discussed above, we have studied the solvent effect on the isotropic hfs's of 4-amino-2,2,6,6-tetramethylpiperid-1-yloxyl (TANINE) shown in Figure 8. Experimental evidence shows that the hcc of ^{14}N increases with the polarity of the solvent. In particular, an increase of 1.77 G is observed when going from *n*-hexane to water.[61] The results obtained at the B3LYP/EPR-2 level, using the geometry optimized in vacuo by the extended MM+ force field and the PCM representation of the solvent, are shown in Table 9. Unfortunately, the hfs in vacuo is not experimentally known, but our computed shift between vacuum and *n*-hexane is quite small, as is expected for low-polarity solvents. A quite large shift is then computed for the passage from *n*-hexane to aqueous solutions (0.96 G), but it remains significantly smaller than the experimental value. It can be argued that continuum solvent models are not sufficient to reproduce the specific effect of the two water molecules discussed above. However, the shift computed for the adduct with two water molecules (1.27 G) is again smaller than the experimental value. A satisfactory agreement with experiment (1.82 vs 1.77 G) can be achieved only by taking into account at the same time bulk and specific solvent effects by a PCM computation of the dihydrated adduct. Note that geometry reoptimization in the presence of the solvent induces only negligible modifications of structural parameters, so that the shift of the hfs's is entirely due to polarization of the solute wave function by the solvent.

A similar, albeit smaller, effect of specific solvation should be obtained for methanol, but a complete analysis of this problem is still in progress since the number of strongly coordinated methanol molecules is quite controversial.[30] In any case, the MM/DF/PCM approach appears very promising for the study of spectroscopic properties in solution. Moreover, the case of nitroxides is quite special due to the particularly large polarizing effect of strongly coordinated water molecules. However, even in this case, the number of water molecules to be explicitly accounted for is relatively small, so that reliable computations remain feasible also for large solutes.

Conclusion

This article is devoted to the development and validation of a combined QM/MM approach for the study of large nitroxide systems both in vacuo and in condensed phases. Our results show that addition of a limited number of parameters to current force fields is sufficient to closely match the reference experimental and quantum mechanical data for prototypical compounds. In particular, substituent effects on the piramidality of the NO moiety can be accounted for by careful consideration of torsional terms. Condensed phases can be described by the same force fields only by taking into proper account the hydrogen bond interactions. We next investigated the reliability of single-point quantum mechanical computations at MM-optimized geometries for the evaluation of spectroscopic parameters. The first results obtained for the magnetic properties of a large biradical and for the solvent effects on the EPR spectrum of a typical nitroxide are very encouraging. Work is in progress in our laboratories to extend these results to other systems and to investigate magnetostructural relationships both in the solid phase and in solution.

Acknowledgment. The financial support of the Italian Research Council (CNR) is gratefully acknowledged.

JA981079Z

(59) Boys, S. F.; Bernardi, F. *Mol. Phys.* **1970**, *19*, 558.
(60) Dixon, R. W.; Kollman, P. A. *J. Comput. Chem.* **1997**, *18*, 1632.
(61) Knauer, B. R.; Napier, J. J. *J. Am. Chem. Soc.* **1976**, *98*, 4395.